

# OPTIMIZE WEIGHT ROUNDING VIA SIGNED GRADIENT DESCENT FOR THE QUANTIZATION OF LLMs

Wenhua Cheng\*, Weiwei Zhang, Haihao Shen, Yiyang Cai, Xin He & Kaokao Lv  
Intel

## ABSTRACT

Large Language Models (LLMs) have proven their exceptional capabilities in performing language-related tasks. However, their deployment poses significant challenges due to their considerable memory and storage requirements. In response to this issue, weight-only quantization, particularly 3 and 4-bit weight-only quantization, has emerged as one of the most viable solutions. As the number of bits decreases, the quantization grid broadens, thus emphasizing the importance of up and down rounding. While previous studies have demonstrated that fine-tuning up and down rounding with the addition of perturbations can enhance accuracy in some scenarios, our study is driven by the precise and limited boundary of these perturbations, where only the threshold for altering the rounding value is of significance. Consequently, we propose a concise and highly effective approach for optimizing the weight rounding task. Our method, named SignRound, involves lightweight block-wise tuning using signed gradient descent, enabling us to achieve outstanding results within 400 steps. SignRound outperforms the established baseline of rounding-to-nearest (RTN) and competes impressively against recent methods, without introducing additional inference overhead. The source code will be publicly available at <https://github.com/intel/neural-compressor> soon.

## 1 INTRODUCTION

Large language models (LLMs) have demonstrated exceptional proficiency on language-related tasks (OpenAI; Touvron et al., 2023a). Nevertheless, the deployment of LLMs presents notable hurdles due to their extensive memory and storage needs. Moreover, the computational demands of these models leads to the challenges for real-time applications. Consequently, it becomes imperative to explore techniques like quantization to facilitate the efficient deployment of LLMs.

Quantization techniques can be broadly classified into two categories: quantization-aware training (QAT) (Esser et al., 2019; Zhuang et al., 2021; Lee et al., 2021; Liu et al., 2023) and post-training quantization (PTQ) (Nagel et al., 2019; Xiao et al., 2022; Frantar et al., 2022; Nagel et al., 2020). QAT involves training the model with quantization in mind. During QAT, the model is trained using simulated lower-precision representations, allowing it to learn and adapt to the effects of quantization. This approach often yields better accuracy compared to PTQ. However, QAT comes with certain drawbacks, including increased training complexity, longer training times, and the need to tune hyperparameters. Applying QAT to LLMs can be particularly costly, despite recent efforts (Hu et al., 2021; Dettmers et al., 2023) to improve the efficiency of fine-tuning LLMs. In contrast, PTQ directly quantizes the model without any simulated training or fine-tuning. While PTQ is a concise approach, it is susceptible to significant accuracy drops, especially with extreme low-bit quantization. This highlights the need for further advancements in PTQ methods to enhance their accuracy preservation capabilities.

Two types of tensors in the neural networks could be quantized: activations and weights. Weight-only quantization has gained prominence in recent times as it offers a favorable tradeoff for LLMs. Quantizing activations for LLMs can be challenging (Wei et al., 2022b; Xiao et al., 2023; Bondarenko et al., 2023), making weight-only quantization a more practical choice. Additionally, the primary bottleneck in generating new tokens for LLMs often lies in memory bandwidth (Kim et al.,

\*Corresponding author wenhua.cheng@intel.com

2023), further emphasizing the significance of weight-only quantization. In this work, we only focus on weight only quantization.

In order to quantize the weights, a rounding operation is necessary, with rounding-to-nearest (RTN) being the predominant method. RTN quantizes each element independently by simply rounding it to the nearest integer. However, RTN fails to consider the relationships between weights and weights, as well as weights and activations. The potential of an advanced rounding strategy to improve accuracy has been initially demonstrated by Nagel et al. (Nagel et al., 2020). They addressed the rounding task by formulating it as a quadratic unconstrained binary optimization problem and approximated the task loss by employing a Taylor series expansion. However, relying exclusively on the second-order term may not produce accurate results. This is because rounding can introduce considerable weight modifications that may make other order terms significant and non-negligible.

We advocate for the use of the signed gradient descent method to effectively tackle the issue of sub-optimal rounding solutions. This approach is inspired by the well-defined boundaries of the solution space, which are confined to the range of  $[-0.5, 0.5]$ , where only the threshold for altering the rounding value is of significance. Figure 1 provides an overview of our method, SignRound. It utilizes signed gradient descent to fine-tune the up and down rounding through block-wise output reconstruction, resulting in enhanced flexibility and faster convergence. Our contributions are primarily twofold:

- We introduce a succinct and potent method for optimizing the weight-rounding task. Our approach utilizes a minimal amount of unlabeled data and executes quantization in a block-wise fashion. Moreover, it is worth noting that our method does not introduce any additional overhead during inference, further enhancing its general practicality.
- Our empirical results exhibit substantial performance enhancements over the established baseline of RTN, and our method contends favorably against recent techniques.

## 2 RELATED WORK

**Quantization Aware Training.** QAT methods have gained widespread popularity in model compression, as they enable the fine-tuning process, often leading to superior accuracy compared to the PTQ method. In their work, (Esser et al., 2019) proposed a novel approach that estimates and scales the task loss gradient at each weight and activation layer’s quantizer step size, allowing for joint learning with other network parameters. (Zhuang et al., 2021) put forward a progressive quantization scheme that involves quantizing activations after weights. Additionally, CPQ (Lee et al., 2021) effectively identified the optimal quantization grids while naturally encouraging the underlying full-precision weights to gather around those quantization grids cohesively during training. While QAT methods are popular in relatively small-scale models, their application in LLMs is limited due to the high computational cost associated with training or fine-tuning.

**Post-training Quantization (PTQ).** PTQ methods simplify the quantization process without the needs of additional training. (Nagel et al., 2019) focused on minimizing quantization error through weight equalization and bias correction techniques. (Liu et al., 2021) specifically addressed the quantization of vision transformers, introducing a ranking loss to preserve the relative order of self-attention results after quantization and exploring a mixed-precision quantization scheme. (Frantar & Alistarh, 2022) leveraged Optimal Brain Surgeon (Hassibi et al., 1993) to tune weights during model compression. Both Hawq (Yao et al., 2021) and HAQ (Wang et al., 2019) aimed to identify important layers and maintain higher precision for them. Given its low resource requirement, PTQ is particularly suitable for the quantization of Large Language Models (LLMs). We will next focus on the quantization methods designed for LLMs, most of which fall under the category of PTQ.

**Large Language Models Quantization.** Significant advancements have been made in addressing the pressing demand for quantizing large language models (LLMs). LLM.int8() (Dettmers et al., 2022) introduced a mixed precision approach to preserve essential channels in high precision. ZeroQuantV2 (Yao et al., 2023) employed low-rank matrices to enhance model quality recovery. RPTQ (Yuan et al., 2023) mitigated the impact of range differences between channel by rearranging the channels and quantizing them in clusters. Other methods, such as SPIQ (Yvinec et al., 2023), SmoothQuant (Xiao et al., 2022), Outlier Suppression+ (Wei et al., 2023), utilized handcrafted

equivalent transformations to mitigate quantization errors. While these approaches are effective, their applicability is limited due to the performance overhead involved during inference, because there is no chance to fuse the transformation scale to the model itself on certain model architectures. LLM-QAT (Liu et al., 2023) employs QAT to enhance the performance of W4A8. In the context of weight-only quantization, GPTQ (Frantar et al., 2022) optimized weights using the Optimal Brain Surgeon (Hassibi et al., 1993) technique, achieving low-bit quantization on LLMs with minimal computational overhead. AWQ (Lin et al., 2023) followed the equivalent transformation approach with additional tuning in a constrained space, and has the similar limitations as SmoothQuant (Xiao et al., 2022). SqueezeLLM (Kim et al., 2023) employed sensitivity-based non-uniform quantization and dense-and-sparse decomposition to achieve lossless compression to ultra-low precision. While recent advancements in LLM quantization have made significant progress, there is still room for improvement in achieving minimal quantization loss without introducing inference overhead.

**Rounding Methods.** Adaptive Rounding (Nagel et al., 2020) has already showcased the potential of an advanced rounding strategy to enhance accuracy (Li et al., 2021; Wei et al., 2022a). They used the rounding task as a quadratic unconstrained binary optimization problem by approximating the task loss through a Taylor series expansion. However, considering only the second-order term may not yield accurate results. This is because the rounding value gets multiplied by a scaling coefficient during de-quantization, potentially introducing significant weight changes that make other order terms non-negligible. FlexRound (Lee et al., 2023) introduces a more flexible approach to rounding by incorporating element-wise division. This allows for simultaneous learning of a shared quantization grid size and individual scales for each pre-trained weight. However, it’s not easily scalable to apply to LLMs due to the needs of specialized hyper-parameters for each specific model and task. AQuant (Li et al., 2022) introduced a dynamic approach where the border becomes a function dependent on the activation value to reduce the quantization error of activation. We specifically concentrate on the up and down rounding task for weight quantization in this work.

**Signed Gradient Descent.** Signed gradient descent is not commonly utilized and is typically applied in specific scenarios, such as reducing communication costs. This is because signed gradient carries significantly less information compared to original gradient. Recent studies have shed light on the advantages of sign-based methods over gradient descent in certain conditions. Safaryan et al. (Safaryan & Richtárik, 2021) found that sign-based methods are preferable when the Hessian matrix is concentrated on its diagonal and the maximal eigenvalue is much larger than the average eigenvalue. Li et al. (Li et al., 2023) investigated a variant of sign-based gradient descent that exhibits faster convergence. Additionally, Safaryan et al. (Safaryan & Richtárik, 2021) proposed a stochastic sign descent with momentum, which converges under the standard bounded variance assumption with the optimal asymptotic rate. These findings contribute to a better understanding of the potential benefits and applications of signed gradient descent methods.

### 3 METHODOLOGY

We provide an overview of quantization before diving into the details of our approach. To quantize and de-quantize the weights, the following operation as shown in Eq.1 is used (disregarding zero point for simplicity).

$$\widetilde{W} = s * clip\left(\left\lfloor \frac{W}{s} \right\rfloor, n, m\right), n, m \in \mathbb{N} \quad (1)$$

where  $s$  is the quantization scale, which is a positive scalar value. However, it is important to mention that our method can be easily extended to cases where  $s$  is a vector or tensor. And the rounding operation  $\lfloor \cdot \rfloor$  is typically performed using the RTN method. While RTN is a concise approach, it quantizes each element independently, thereby losing the ability to model the correlation among different weights or activations.

To introduce more flexibility into the rounding operation, a tensor  $V$  with the same shape of  $W$  is introduced. Each element of  $V$  falls within the range of  $[-B, B]$ , in which  $B$  is set to 0.5 in all of experiments to ensure that the changes made only impact the rounding value.

$$\widetilde{W} = s * clip\left(\left\lfloor \frac{W}{s} + V \right\rfloor, n, m\right), n, m \in \mathbb{N} \quad (2)$$

This adjustment allows for a more adaptable and context-aware quantization process. if we try to reconstruct the output of layers, the loss could be formulated as

$$L = \|WX - \widetilde{W}X\|_F^2 \quad (3)$$

where  $X$  is the input of the layer and  $\|\cdot\|_F$  denotes the Frobenius norm. Then the final optimization task is described as:

$$\arg \min_V \|WX - \widetilde{W}X\|_F^2 \quad (4)$$

### 3.1 SIGNROUND

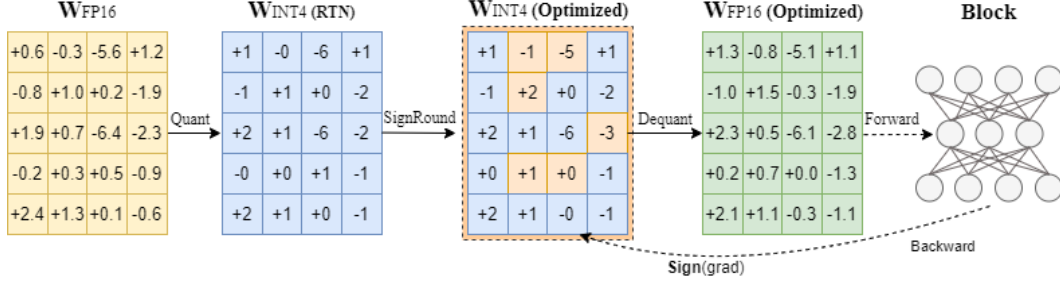


Figure 1: An illustration of SignRound. Unlike the direct rounding in RTN, SignRound performs signed gradient descent to fine-tune the up and down rounding through block-wise output reconstruction. After lightweight forward and backward steps,  $\mathbf{W}_{\text{INT4}}$  has been well optimized towards the minimal loss, therefore ready for the final inference deployment. Note that Quant and Dequant are two standard operations for quantization and dequantization respectively.

Since  $V$  has a clear boundary, i.e.  $[-0.5, 0.5]$ , we prefer scaled signed gradient descent instead of normal gradient descent to optimize this task. Figure 1 shows an illustration of our method. More precisely, we follow the below optimization to approach the sub-optimal solution of Eq. 4.

$$\begin{aligned} V_{t+1} &= V_t - lr * \text{sign}\left(\frac{\partial L}{\partial V}\right) \\ \text{s.t.} & \left| \sum_t lr * \text{sign}\left(\frac{\partial L}{\partial V}\right) \right| \leq B \end{aligned} \quad (5)$$

where  $t$  is the optimizing step,  $lr$  is the learning rate,  $|\cdot|$  is the absolute operation and  $B$  is the boundary we use, which is set to 0.5 in all our experiments.

Further, by employing straight-through estimator (STE) (Bengio et al., 2013), it can be easily demonstrated that  $\text{sign}\left(\frac{\partial L}{\partial V}\right) = \text{sign}\left(\frac{\partial L}{\partial W}\right)$  in Eq. 5 as following since elements of  $s$  are all positive.

$$\frac{\partial L}{\partial W} = -2(WX - \widetilde{W}X)X^T \quad (6)$$

$$\frac{\partial L}{\partial V} = -2s(WX - \widetilde{W}X)X^T \quad (7)$$

So our optimization could be simplified as

$$\begin{aligned} V_{t+1} &= V_t - lr * \text{sign}\left(\frac{\partial L}{\partial W}\right) \\ \text{s.t.} & \left| \sum_t lr * \text{sign}\left(\frac{\partial L}{\partial W}\right) \right| \leq B \end{aligned} \quad (8)$$

Moreover, as Eq 3 averages the loss of each element, which presumes that each one contributes equally to the network, that basically is not true. To alleviate this issue, we optimize the rounding

task blockwise. To clarify, in our context, we use the term 'layer' to refer to a linear/convolution layer, while 'block' denotes a transformer block that typically consists of several linear layers.

The below pseudocode 1 presents more details of SignRound.

---

**Algorithm 1** SignRound

---

**Input:** Calibration Data  $\mathcal{D}$ , learning rate  $lr$ , total steps  $T$ , Model  $M$ , block module  $m_w$  with weights  $w$ , zero initialized  $V$ , batch size  $bs$

**Output:**  $best\_V$

```

1:  $V \leftarrow 0, best\_V \leftarrow 0, best\_l \leftarrow maximum$ 
2: for  $i \leftarrow 0$  to  $T$  do
3:    $d \leftarrow draw\ bs\ samples\ from\ \mathcal{D}$ 
4:    $x \leftarrow M(d)_m$  ▷ gets the inputs of m
5:    $y_f \leftarrow m_w(x)$  ▷ get the output of original module
6:    $\tilde{w} \leftarrow qdq(w, V)$  ▷ quantize and dequantize w via Eq.2
7:    $y_q \leftarrow m_{\tilde{w}}(x)$  ▷ get the output of quantized module
8:    $loss \leftarrow mse(y_q, y_f)$  ▷ get the loss via Eq.3
9:   if  $loss < best\_l$  then
10:      $best\_V \leftarrow V$ 
11:      $best\_l \leftarrow loss$ 
12:   end if
13:    $loss.backward()$ 
14:    $update\ V\ via\ Eq8$ 
15: end for

```

---

## 4 EXPERIMENTS

In this section, we conduct a comprehensive evaluation of SignRound from various perspectives. Firstly, we provide a brief overview of the LLM architectures and tasks that are included in our evaluation. Secondly, we present a detailed comparison between our method and other existing approaches, highlighting the unique features and advantages of SignRound. Thirdly, we conduct additional experiments to further demonstrate the validity of our choices, assess the sensitivity of hyperparameters, and explore other relevant factors.

### 4.1 EXPERIMENTAL SETTINGS

**Evaluation and Datasets.** We make assessments on several language tasks to satisfy the task-agnostic setting. Specifically, we report average accuracy results on four common sense reasoning tasks by leveraging lm-eval-harness(Gao et al., 2021), including HellaSwag (Zellers et al., 2019), WinoGrande (Sakaguchi et al., 2021), PIQA (Bisk et al., 2020) and LAMBADA (Paperno et al., 2016). Furthermore, we complement our evaluation with perplexity (PPL) analysis on WikiText2 (Merity et al., 2016) and C4 (Raffel et al., 2020), by following the source code <sup>1</sup> of GPTQ.

**Quantization Configurations.** In line with the approach taken in GPTQ (Frantar et al., 2022), we specifically concentrate on weight-only quantization, targeting the linear layers within transformer blocks. Other layers, such as the embedding layer and typically the last layer like lm-head, are excluded from the quantization process. We initially intended to utilize the pile dataset for calibration, following AWQ (Lin et al., 2023) and SmoothQuant(Xiao et al., 2022). However, due to its large size, we have opted to use the readily available pile-10k dataset <sup>2</sup>, which consists of the first 10k samples from pile, for both GPTQ and our method. We employ standard uniform per-row asymmetric quantization on the min-max grid. Our evaluation primarily revolves around W4, W4G128, and W3G128, where W4 indicates quantizing weights with 4 bits and G represents finer-granularity grouping as described in (Park et al., 2022; Frantar et al., 2022).

<sup>1</sup><https://github.com/IST-DASLab/gptq>

<sup>2</sup><https://huggingface.co/datasets/NeelNanda/pile-10k>

**Large Language Models.** Our experimental evaluation encompasses a range of widely adopted LLM architectures, such as LLaMAs (Touvron et al., 2023a), LLaMAs v2 (Touvron et al., 2023b), BLOOMs (Scao et al., 2022), and OPTs (Zhang et al., 2022). We cover a broad spectrum of parameter scalings, ranging from millions to billions, to ensure comprehensive coverage and analysis.

**SignRound Hyperparameters.** To create our tuning dataset, we selected 512 samples randomly from pile-10k and truncated each sample to a sequence length of 256. The tuning process involves adjusting each block for 400 steps using a learning rate of  $2.5e-3$ , a batch size of 8, and employing a linear learning rate decay. In Equation 8, we set the value of B to 0.5, ensuring that we only modify the rounding value by  $\pm 1$ .

Table 1: Average % accuracy( $\uparrow$ ) of HellaSwag, WinoGrand, PIQA and LAMBADA for LLaMA & OPT.

nbits	methods	LLaMA				OPT				
		7b	13b	7bv2	13bv2	125m	1.3b	2.7b	6.7b	13b
16	FP16	68.80	71.14	69.02	71.20	45.09	57.66	61.04	64.92	65.49
W4	RTN	67.38	68.82	66.98	70.17	39.41	47.22	58.61	62.99	64.08
	GPTQ	64.70	70.00	66.89	69.24	43.58	56.15	59.92	63.09	<b>64.83</b>
	Ours	<b>67.64</b>	<b>70.62</b>	<b>67.96</b>	<b>70.30</b>	<b>43.85</b>	<b>56.82</b>	<b>60.57</b>	<b>64.55</b>	64.68
W4G128	RTN	67.85	70.84	68.32	70.72	<b>45.27</b>	56.47	60.70	64.03	64.84
	GPTQ	66.32	<b>70.92</b>	<b>68.90</b>	70.68	42.88	56.99	61.23	<b>64.75</b>	65.37
	Ours	<b>67.96</b>	70.89	68.59	<b>70.81</b>	44.76	<b>57.55</b>	<b>61.52</b>	64.71	<b>65.57</b>
W3G128	RTN	64.94	67.70	65.92	68.70	39.11	42.61	36.99	56.09	49.56
	GPTQ	64.70	68.73	61.87	68.73	39.78	54.43	58.47	<b>62.98</b>	<b>64.68</b>
	Ours	<b>66.31</b>	<b>69.38</b>	<b>66.63</b>	<b>69.79</b>	<b>43.46</b>	<b>55.63</b>	<b>59.28</b>	57.76	64.49

Table 2: Average % accuracy( $\uparrow$ ) of HellaSwag, WinoGrand, PIQA and LAMBADA for BLOOM.

Size	W4				W4G128				W3G128			
	560m	1b7	3b	7b1	560m	1b7	3b	7b1	560m	1b7	3b	7b1
FP16	45.50	52.31	55.48	60.22	45.50	52.31	55.48	60.22	45.50	52.31	55.48	60.22
RTN	43.10	49.97	53.16	57.73	44.28	<b>52.08</b>	54.86	59.31	40.83	47.98	52.51	57.59
GPTQ	43.95	50.91	<b>54.65</b>	58.27	44.79	<b>52.08</b>	<b>55.68</b>	59.59	42.74	48.81	53.41	58.12
Ours	<b>44.81</b>	<b>51.71</b>	54.32	<b>59.08</b>	<b>44.94</b>	51.86	55.22	<b>59.90</b>	<b>44.39</b>	<b>50.10</b>	<b>53.82</b>	<b>58.34</b>

## 4.2 COMPARING WITH OTHER METHODS

We conducted a comprehensive benchmarking of our results against RTN and GPTQ (Frantar et al., 2022). However, it is important to highlight that act-order was not enabled in GPTQ due to the kernel overhead it introduces (Lin et al., 2023), although it has the potential to improve accuracy for certain models. In our evaluation, we prioritize reporting the C4 perplexity (ppl) as our primary focus, taking into consideration the potential occurrence of NaN values when assessing perplexity for wikitext2 and ptb datasets, both for our model and GPTQ. Furthermore, we conducted a limited and non-rigorous comparison between our approach and AWQ Lin et al. (2023) in Appendix A.1.

We begin by presenting the average accuracy results for the HellaSwag, WinoGrand, PIQA, and LAMBADA tasks across LLaMA, OPT, and BLOOM models with a size below 13B. These results are tabulated in Table 1 and 2. In conclusion, our method consistently outperforms RTN in 37 out of 39 scenarios, showcasing its effectiveness. It is worth noting that GPTQ does not surpass RTN in the remaining 2 scenarios either. Additionally, when comparing our approach to GPTQ, we surpass it in 30 out of 39 scenarios, further highlighting the strengths of our method. While our method showcases overall effectiveness, it is important to acknowledge the presence of outliers, such as OPT6.7B at W3G128. Although the root cause for this has not been identified yet, it could be mitigated by fine-tuning hyperparameters, as discussed in the following sections. Notably, when comparing to W4G128, our approach exhibits more advantages in W4 and W3G128. This can be attributed to two reasons. Firstly, both RTN and GPTQ perform relatively strongly in W4G128,

leading to less significant differences between each method. Secondly, as mentioned in the abstract, the decrease in quantization bits places a greater emphasis on rounding.

We then present the perplexity (ppl) results for C4 in Table 3, along with the detailed results for Wikitext2 in Appendix A.2. In conclusion, our performance is comparable to that of GPTQ. In certain cases where the results may not be optimal, we can still fine-tune the hyperparameters to achieve better results, as demonstrated in the subsequent sections.

We also provide the results for models with a capacity of 30B or greater at W3G128 in Table 4 and W4 in Appendix A.3. Additionally, we discovered that modifying the sequence length to 512 of the calibration dataset yielded improvements in certain scenarios, and thus we include these results. In summary, our approach achieves comparable performance to GPTQ for the given accuracy task. However, we slightly lag behind GPTQ in terms of PPL tasks.

Table 3: C4 ppl ( $\downarrow$ ) at W4.

Size	LLaMA				OPT				BLOOM			
	7b	13b	7bv2	13bv2	1.3b	2.7b	6.7b	13b	560m	1b7	3b	7b1
FP16	7.34	6.80	7.26	6.73	16.07	14.34	12.71	12.06	26.59	19.49	17.48	15.20
RTN	8.12	7.23	8.16	7.14	27.49	18.83	14.37	13.32	29.87	21.25	18.76	16.05
GPTQ	8.64	7.13	<b>7.90</b>	<b>6.87</b>	17.04	15.06	13.39	<b>12.29</b>	<b>28.15</b>	20.71	<b>18.18</b>	<b>15.67</b>
Ours	<b>7.81</b>	<b>7.07</b>	8.19	7.23	<b>16.94</b>	<b>14.98</b>	<b>13.10</b>	12.53	28.18	<b>20.43</b>	18.24	15.71

Table 4: Average % accuracy( $\uparrow$ ) of HellaSwag, WinoGrand, PIQA and LAMBADA and C4 ppl( $\downarrow$ ) for LLaMA & OPT with  $\geq 30B$  at W3G128. "Ours-seq512" indicates that we have modified the sequence length of the calibration dataset from 256 to 512.

Type	Accuracy				PPL on C4			
	LLaMA		OPT		LLaMA		OPT	
	30b	65b	30b	66b	30b	65b	30b	66b
FP16	73.46	75.48	67.87	69.54	6.13	5.98	11.46	10.99
RTN	72.17	73.69	62.83	38.00	6.85	6.52	30.81	285.41
GPTQ	72.09	<b>73.97</b>	<b>66.76</b>	67.87	6.80	6.52	<b>11.74</b>	<b>11.87</b>
Ours	<b>72.45</b>	73.71	66.51	<b>68.01</b>	6.83	<b>6.52</b>	13.00	13.34
Ours-seq512	72.00	73.78	66.70	67.26	<b>6.79</b>	6.53	12.50	13.97

### 4.3 BLOCK-WISE VERSUS LAYER-WISE

We examined the effects of layer-wise and block-wise tuning. As explained in Section 3.1, the term "layer" refers to a linear/convolution layer, while "block" specifically denotes a transformer block consisting of multiple linear layers. Based on the results, block-wise tuning outperformed layer-wise tuning in the majority of scenarios.

Table 5: Comparing block-wise and layer-wise tuning for around 7B models, the models LLaMA7b, LLaMA7bv2, OPT6.7b, and BLOOM7b1 are denoted by 7b, 7bv2, 6.7b, and 7b1 respectively. The accuracy is the % average accuracy( $\uparrow$ ) of HellaSwag, WinoGrand, PIQA and LAMBADA . Perplexity (PPL) ( $\downarrow$ ) is evaluated using the C4 dataset.

Size	W4				W3G128			
	7b	7bv2	6.7b	7b1	7b	7bv2	6.7b	7b1
layer-acc	67.50	67.78	63.46	58.72	65.96	66.09	<b>61.60</b>	58.24
block-acc	<b>67.64</b>	<b>67.96</b>	<b>64.55</b>	<b>59.08</b>	<b>66.31</b>	<b>66.63</b>	57.76	<b>58.34</b>
layer-c4-ppl	8.02	<b>7.92</b>	13.44	15.73	8.81	<b>8.69</b>	<b>16.83</b>	16.15
block-c4-ppl	<b>7.81</b>	8.19	<b>13.10</b>	<b>15.71</b>	<b>8.34</b>	10.84	25.44	<b>16.05</b>

#### 4.4 THE ANALYSIS OF HYPERPARAMETERS SENSITIVITY

We conducted a hyperparameters sensitivity analysis, the results of which are summarized in Table 6. In the "steps100" configuration, we used 100 steps, a batch size of 32, and a learning rate of  $1e-2$ . For the "steps200" configuration, we employed 200 steps, a batch size of 16, and a learning rate of  $5e-3$ . In the "lr3e-3" configuration, we set the learning rate to  $3e-3$ , while in the "lr4e-4" configuration, the learning rate was  $4e-3$ . Please note that all other hyperparameters not mentioned in each configuration were kept the same as the default configurations, as detailed in Section 4.1. In general, our method demonstrates robustness to hyperparameters in most scenarios.

Table 6: Hyperparameter sensitivity analysis, the models LLaMA7b, LLaMA7bv2, OPT6.7b, and BLOOM7b1 are denoted by 7b, 7bv2, 6.7b, and 7b1 respectively. The accuracy is the % average accuracy( $\uparrow$ ) of HellaSwag, WinoGrand, PIQA and LAMBADA . Perplexity (PPL) ( $\downarrow$ ) is evaluated using the C4 dataset.

Size	Accuracy				PPL on C4			
	7b	7bv2	6.7b	7b1	7b	7bv2	6.7b	7b1
steps100	67.75	67.70	64.30	59.04	7.93	<b>7.84</b>	13.09	15.73
steps200	<b>68.13</b>	67.96	64.64	59.31	7.92	8.65	13.11	15.73
lr3e-3	67.55	67.53	<b>64.79</b>	59.08	7.90	8.95	<b>13.08</b>	15.72
lr4e-3	67.42	<b>68.16</b>	64.55	<b>59.37</b>	7.93	8.25	13.10	15.72
default	67.64	67.96	64.55	59.08	<b>7.81</b>	8.19	13.10	<b>15.71</b>

#### 4.5 ANALYSIS OF GRADIENTS AND THEIR EFFECTS ON ROUNDING

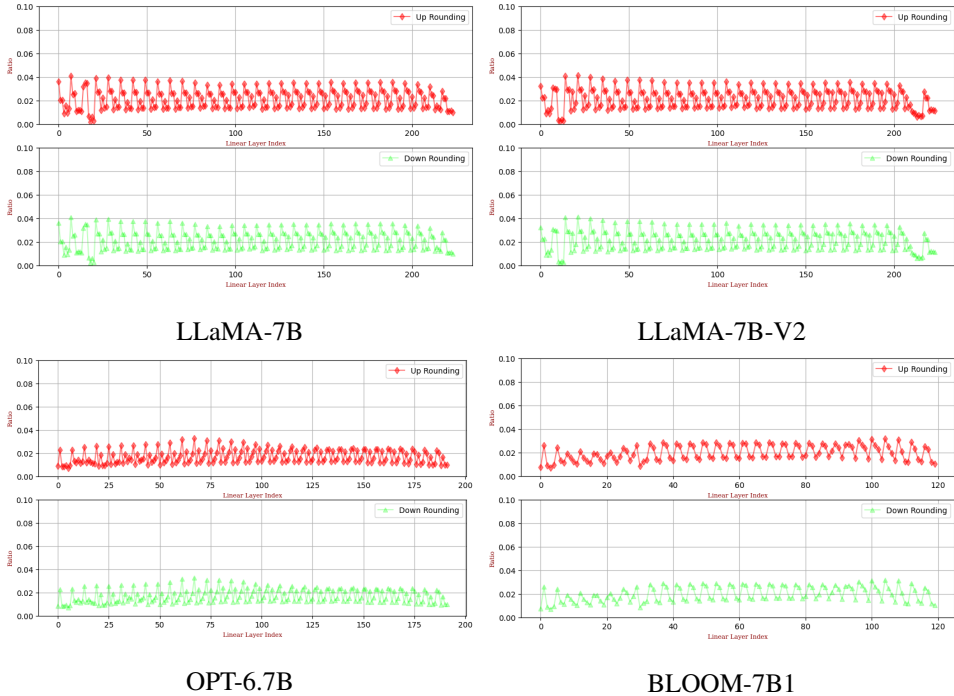


Figure 2: The impact of the rounding value introduced by the  $V$  in Eq. 2

In this analysis, we dive into the distribution of the magnitude of  $V$  in Eq. 2 and its impact on rounding values across a dataset of approximately 7 billion models at W4. The visual representations of these distributions are provided in Appendix A.4. Our investigation reveals that the majority of  $V$  values are concentrated within the range of  $[-0.3, 0.3]$ . Additionally, we observe an interesting pattern in the distribution of  $V$  across different layers. The middle layers exhibit a more tightly



clustered distribution compared to the other layers. This observation aligns with the common understanding that the head and tail layers tend to be more sensitive to compression, while the middle layers are relatively more robust.

Figure 2 illustrates the impact of the rounding value introduced by the  $V$  in Eq. 2 for models around 7B at W4. The red line represents "up rounding", indicating that while RTN rounds the value to the floor, Sign round changes it to the ceiling. Conversely, the green line represents "down rounding" indicating that while RTN rounds the value to the ceiling, SignRound changes it to the floor. Notably, it is evident that SignRound only alters less than 8% of all rounding values for weights.

We were also intrigued by the possible correlation between rounding and activation, as previous research has shown that keeping only 0.1%-1% of the channels corresponding to larger activation can significantly improve the quantized performance in AWQ (Lin et al., 2023). Therefore, we investigated whether the altered rounding values tend to fall more frequently in these salient channels. The results of our analysis, presented in Figure 3, reveal an interesting finding. The ratio, representing the percentage of altered rounding values falling within the top 1% salient activation channels out of all altered rounding values, is typically around 1%. This suggests that there is no strong correlation between rounding and activation. It is possible that rounding values of less significant channels need to be changed more to compensate for the quantization error introduced by these salient channels.

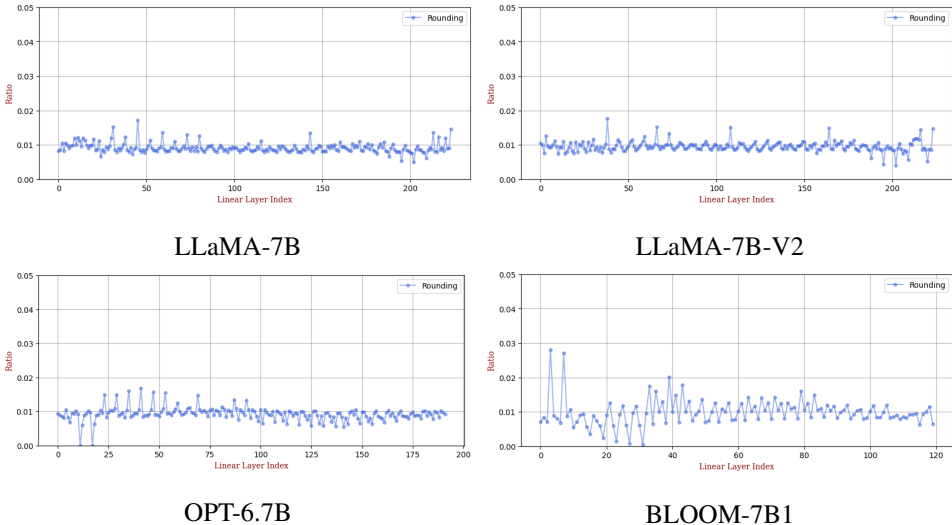


Figure 3: The correction between SignRound and salient activation channels

## 5 CONCLUSION AND LIMITATIONS

In this paper, we present a highly effective and concise approach to optimize the weight rounding task. Our method, SignRound, leverages lightweight block-wise tuning using signed gradient descent, achieving remarkable results within a mere 400 steps. Extensive experiments demonstrate the superior performance of our approach. As part of our future work, we plan to apply our approach to more diverse LLM models (e.g., Code LLaMA Rozière et al. (2023), LLaMA v2 Chat Touvron et al. (2023b)), and contribute our recipes and implementations to the open source community. On the other hand, although our method is generally effective, there are a few outliers in certain scenarios, where we plan to mitigate the issue by fine-tuning the hyper-parameters.

## REFERENCES

Yoshua Bengio, Nicholas Léonard, and Aaron Courville. Estimating or propagating gradients through stochastic neurons for conditional computation. *arXiv preprint arXiv:1308.3432*, 2013.

- Yonatan Bisk, Rowan Zellers, Jianfeng Gao, Yejin Choi, et al. Piqa: Reasoning about physical commonsense in natural language. In *Proceedings of the AAAI conference on artificial intelligence*, volume 34, pp. 7432–7439, 2020.
- Yelysei Bondarenko, Markus Nagel, and Tijmen Blankevoort. Quantizable transformers: Removing outliers by helping attention heads do nothing. *arXiv preprint arXiv:2306.12929*, 2023.
- Tim Dettmers, Mike Lewis, Younes Belkada, and Luke Zettlemoyer. Llm.int8(): 8-bit matrix multiplication for transformers at scale. *arXiv preprint arXiv:2208.07339*, 2022.
- Tim Dettmers, Artidoro Pagnoni, Ari Holtzman, and Luke Zettlemoyer. Qlora: Efficient finetuning of quantized llms. *arXiv preprint arXiv:2305.14314*, 2023.
- Steven K Esser, Jeffrey L McKinstry, Deepika Bablani, Rathinakumar Appuswamy, and Dharmendra S Modha. Learned step size quantization. *arXiv preprint arXiv:1902.08153*, 2019.
- Elias Frantar and Dan Alistarh. Optimal brain compression: A framework for accurate post-training quantization and pruning. *arXiv preprint arXiv:2208.11580*, 2022.
- Elias Frantar, Saleh Ashkboos, Torsten Hoefler, and Dan Alistarh. Gptq: Accurate post-training quantization for generative pre-trained transformers. *arXiv preprint arXiv:2210.17323*, 2022.
- Leo Gao, Jonathan Tow, Stella Biderman, Sid Black, Anthony DiPofi, Charles Foster, Laurence Golding, Jeffrey Hsu, Kyle McDonell, Niklas Muennighoff, Jason Phang, Laria Reynolds, Eric Tang, Anish Thite, Ben Wang, Kevin Wang, and Andy Zou. A framework for few-shot language model evaluation, September 2021. URL <https://doi.org/10.5281/zenodo.5371628>.
- Babak Hassibi, David G Stork, and Gregory J Wolff. Optimal brain surgeon and general network pruning. In *IEEE international conference on neural networks*, pp. 293–299. IEEE, 1993.
- Edward J Hu, Yelong Shen, Phillip Wallis, Zeyuan Allen-Zhu, Yuanzhi Li, Shean Wang, Lu Wang, and Weizhu Chen. Lora: Low-rank adaptation of large language models. *arXiv preprint arXiv:2106.09685*, 2021.
- Sehoon Kim, Coleman Hooper, Amir Gholami, Zhen Dong, Xiuyu Li, Sheng Shen, Michael W Mahoney, and Kurt Keutzer. Squeezellm: Dense-and-sparse quantization. *arXiv preprint arXiv:2306.07629*, 2023.
- Jung Hyun Lee, Jihun Yun, Sung Ju Hwang, and Eunho Yang. Cluster-promoting quantization with bit-drop for minimizing network quantization loss. In *Proceedings of the IEEE/CVF International Conference on Computer Vision*, pp. 5370–5379, 2021.
- Jung Hyun Lee, Jeonghoon Kim, Se Jung Kwon, and Dongsoo Lee. Flexround: Learnable rounding based on element-wise division for post-training quantization. *arXiv preprint arXiv:2306.00317*, 2023.
- Xiuxian Li, Kuo-Yi Lin, Li Li, Yiguang Hong, and Jie Chen. On faster convergence of scaled sign gradient descent. *IEEE Transactions on Industrial Informatics*, 2023.
- Yuhang Li, Ruihao Gong, Xu Tan, Yang Yang, Peng Hu, Qi Zhang, Fengwei Yu, Wei Wang, and Shi Gu. Brecq: Pushing the limit of post-training quantization by block reconstruction. *arXiv preprint arXiv:2102.05426*, 2021.
- Zhengyi Li, Cong Guo, Zhanda Zhu, Yangjie Zhou, Yuxian Qiu, Xiaotian Gao, Jingwen Leng, and Minyi Guo. Efficient activation quantization via adaptive rounding border for post-training quantization. *arXiv preprint arXiv:2208.11945*, 2022.
- Ji Lin, Jiaming Tang, Haotian Tang, Shang Yang, Xingyu Dang, and Song Han. Awq: Activation-aware weight quantization for llm compression and acceleration. *arXiv preprint arXiv:2306.00978*, 2023.
- Zechun Liu, Barlas Oguz, Changsheng Zhao, Ernie Chang, Pierre Stock, Yashar Mehdad, Yangyang Shi, Raghuraman Krishnamoorthi, and Vikas Chandra. Llm-qat: Data-free quantization aware training for large language models. *arXiv preprint arXiv:2305.17888*, 2023.

- Zhenhua Liu, Yunhe Wang, Kai Han, Wei Zhang, Siwei Ma, and Wen Gao. Post-training quantization for vision transformer. *Advances in Neural Information Processing Systems*, 34:28092–28103, 2021.
- Stephen Merity, Caiming Xiong, James Bradbury, and Richard Socher. Pointer sentinel mixture models. *arXiv preprint arXiv:1609.07843*, 2016.
- Markus Nagel, Mart van Baalen, Tijmen Blankevoort, and Max Welling. Data-free quantization through weight equalization and bias correction. In *Proceedings of the IEEE/CVF International Conference on Computer Vision*, pp. 1325–1334, 2019.
- Markus Nagel, Rana Ali Amjad, Mart Van Baalen, Christos Louizos, and Tijmen Blankevoort. Up or down? adaptive rounding for post-training quantization. In *International Conference on Machine Learning*, pp. 7197–7206. PMLR, 2020.
- OpenAI. Openai: Chatgpt. URL <https://openai.com/blog/chatgpt>.
- Denis Paperno, Germán Kruszewski, Angeliki Lazaridou, Quan Ngoc Pham, Raffaella Bernardi, Sandro Pezzelle, Marco Baroni, Gemma Boleda, and Raquel Fernández. The lambada dataset: Word prediction requiring a broad discourse context. *arXiv preprint arXiv:1606.06031*, 2016.
- Gunho Park, Baeseong Park, Se Jung Kwon, Byeongwook Kim, Youngjoo Lee, and Dongsoo Lee. nuqmm: Quantized matmul for efficient inference of large-scale generative language models. *arXiv preprint arXiv:2206.09557*, 2022.
- Colin Raffel, Noam Shazeer, Adam Roberts, Katherine Lee, Sharan Narang, Michael Matena, Yanqi Zhou, Wei Li, and Peter J Liu. Exploring the limits of transfer learning with a unified text-to-text transformer. *The Journal of Machine Learning Research*, 21(1):5485–5551, 2020.
- Baptiste Rozière, Jonas Gehring, Fabian Gloeckle, Sten Sootla, Itai Gat, Xiaoqing Ellen Tan, Yossi Adi, Jingyu Liu, Tal Remez, Jérémy Rapin, et al. Code llama: Open foundation models for code. *arXiv preprint arXiv:2308.12950*, 2023.
- Mher Safaryan and Peter Richtárik. Stochastic sign descent methods: New algorithms and better theory. In *International Conference on Machine Learning*, pp. 9224–9234. PMLR, 2021.
- Keisuke Sakaguchi, Ronan Le Bras, Chandra Bhagavatula, and Yejin Choi. Winogrande: An adversarial winograd schema challenge at scale. *Communications of the ACM*, 64(9):99–106, 2021.
- Teven Le Scao, Angela Fan, Christopher Akiki, Ellie Pavlick, Suzana Ilić, Daniel Hesslow, Roman Castagné, Alexandra Sasha Luccioni, François Yvon, Matthias Gallé, et al. Bloom: A 176b-parameter open-access multilingual language model. *arXiv preprint arXiv:2211.05100*, 2022.
- Hugo Touvron, Thibaut Lavril, Gautier Izacard, Xavier Martinet, Marie-Anne Lachaux, Timothée Lacroix, Baptiste Rozière, Naman Goyal, Eric Hambro, Faisal Azhar, et al. Llama: Open and efficient foundation language models. *arXiv preprint arXiv:2302.13971*, 2023a.
- Hugo Touvron, Louis Martin, Kevin Stone, Peter Albert, Amjad Almahairi, Yasmine Babaei, Nikolay Bashlykov, Soumya Batra, Prajjwal Bhargava, Shruti Bhosale, et al. Llama 2: Open foundation and fine-tuned chat models. *arXiv preprint arXiv:2307.09288*, 2023b.
- Kuan Wang, Zhijian Liu, Yujun Lin, Ji Lin, and Song Han. Haq: Hardware-aware automated quantization with mixed precision. In *Proceedings of the IEEE/CVF conference on computer vision and pattern recognition*, pp. 8612–8620, 2019.
- Xiuying Wei, Ruihao Gong, Yuhang Li, Xianglong Liu, and Fengwei Yu. Qdrop: randomly dropping quantization for extremely low-bit post-training quantization. *arXiv preprint arXiv:2203.05740*, 2022a.
- Xiuying Wei, Yunchen Zhang, Xiangguo Zhang, Ruihao Gong, Shanghang Zhang, Qi Zhang, Fengwei Yu, and Xianglong Liu. Outlier suppression: Pushing the limit of low-bit transformer language models. *Advances in Neural Information Processing Systems*, 35:17402–17414, 2022b.

- Xiuying Wei, Yunchen Zhang, Yuhang Li, Xiangguo Zhang, Ruihao Gong, Jinyang Guo, and Xianlong Liu. Outlier suppression+: Accurate quantization of large language models by equivalent and optimal shifting and scaling. *arXiv preprint arXiv:2304.09145*, 2023.
- Guangxuan Xiao, Ji Lin, Mickael Seznec, Julien Demouth, and Song Han. Smoothquant: Accurate and efficient post-training quantization for large language models. *arXiv preprint arXiv:2211.10438*, 2022.
- Guangxuan Xiao, Ji Lin, Mickael Seznec, Hao Wu, Julien Demouth, and Song Han. Smoothquant: Accurate and efficient post-training quantization for large language models. In *International Conference on Machine Learning*, pp. 38087–38099. PMLR, 2023.
- Zhewei Yao, Zhen Dong, Zhangcheng Zheng, Amir Gholami, Jiali Yu, Eric Tan, Leyuan Wang, Qijing Huang, Yida Wang, Michael Mahoney, et al. Hawq-v3: Dyadic neural network quantization. In *International Conference on Machine Learning*, pp. 11875–11886. PMLR, 2021.
- Zhewei Yao, Xiaoxia Wu, Cheng Li, Stephen Youn, and Yuxiong He. Zeroquant-v2: Exploring post-training quantization in llms from comprehensive study to low rank compensation. *arXiv:2303.08302*, 2023.
- Zhihang Yuan, Lin Niu, Jiawei Liu, Wenyu Liu, Xinggang Wang, Yuzhang Shang, Guangyu Sun, Qiang Wu, Jiayang Wu, and Bingzhe Wu. Rptq: Reorder-based post-training quantization for large language models. *arXiv preprint arXiv:2304.01089*, 2023.
- Edouard Yvinec, Arnaud Dapogny, Matthieu Cord, and Kevin Bailly. Spiq: Data-free per-channel static input quantization. In *Proceedings of the IEEE/CVF Winter Conference on Applications of Computer Vision*, pp. 3869–3878, 2023.
- Rowan Zellers, Ari Holtzman, Yonatan Bisk, Ali Farhadi, and Yejin Choi. Hellaswag: Can a machine really finish your sentence? *arXiv preprint arXiv:1905.07830*, 2019.
- Susan Zhang, Stephen Roller, Naman Goyal, Mikel Artetxe, Moya Chen, Shuohui Chen, Christopher Dewan, Mona Diab, Xian Li, Xi Victoria Lin, et al. Opt: Open pre-trained transformer language models. *arXiv preprint arXiv:2205.01068*, 2022.
- Bohan Zhuang, Mingkui Tan, Jing Liu, Lingqiao Liu, Ian Reid, and Chunhua Shen. Effective training of convolutional neural networks with low-bitwidth weights and activations. *IEEE Transactions on Pattern Analysis and Machine Intelligence*, 44(10):6140–6152, 2021.

## A APPENDIX

### A.1 NON-RIGOROUS COMPARISON WITH AWQ

We conducted a limited comparison between our approach and AWQ Lin et al. (2023), considering that our evaluation methodology closely follows that of GPTQ and we only share a few common tasks with AWQ. It is important to acknowledge that this comparison inherently lacks rigor due to our reliance on referencing AWQ’s data alone. Consequently, this approach introduces the possibility of unfairness in the evaluation process, primarily stemming from the utilization of different calibration datasets and other potential factors that may influence the obtained results.

We present the results of our common tasks alongside AWQ in table 7 and all the results of AWQ are from their paper.

### A.2 RESULTS OF WIKITEXT2 PPL AT W4

The perplexity results for Wikitext2 at W4 are shown in Table 8. In conclusion, our performance is comparable to that of GPTQ.

Table 7: Reported results of AWQ and Ours

LLaMA-7B		AWQ			Ours		
nbits	Method	PIQA	Hella.	Wino.	PIQA	Hella.	Wino.
16	FP16	78.35	56.44	67.09	78.35	56.42	66.85
W3G128	RTN	75.84	53.10	63.22	75.73	53.17	63.14
	GPTQ	70.89	46.77	60.93	72.58	47.10	59.91
	Proposed	76.66	53.63	66.14	76.99	54.22	63.46
W4G128	RTN	77.86	55.81	65.59	77.58	55.86	65.75
	GPTQ	77.20	53.98	65.67	77.26	54.09	64.09
	Proposed	78.07	55.76	65.82	78.07	56.18	65.43

Table 8: Wikitext2 ppl ( $\downarrow$ ) at W4

Size	LLaMA				OPT				BLOOM			
	7b	13b	7bv2	13bv2	1.3b	2.7b	6.7b	13b	560m	1b7	3b	7b1
FP16	5.67	5.09	5.47	4.88	14.62	12.47	10.86	10.13	22.41	15.39	13.48	11.37
RTN	6.29	5.53	6.12	5.20	48.20	16.92	12.10	11.32	25.88	16.97	14.75	12.10
GPTQ	6.59	5.33	<b>6.09</b>	<b>5.16</b>	15.67	13.30	11.59	<b>10.33</b>	<b>23.95</b>	16.37	<b>14.10</b>	<b>11.73</b>
Ours	<b>6.17</b>	<b>5.30</b>	17.87	6.35	<b>15.54</b>	<b>13.09</b>	<b>11.16</b>	10.61	<b>23.95</b>	<b>16.23</b>	14.17	11.82

### A.3 OTHER RESULTS FOR LARGE MODELS

We present the results for models with a capacity of 30B or higher at W4 in Table 9 and PPL on wikitext2 in Table 10. Furthermore, we observed that adjusting the sequence length of the calibration dataset led to improvements in specific scenarios, and we include these findings in our analysis. Overall, our approach demonstrates comparable accuracy performance to GPTQ for the given task. However, it is worth noting that we slightly fall behind GPTQ in terms of PPL tasks.

Table 9: Average % accuracy( $\uparrow$ ) of HellaSwag, WinoGrand, PIQA and LAMBADA and C4 ppl( $\downarrow$ ) for LLaMA & OPT with size  $\geq 30B$  at W4. "Ours-seq512" indicates that we have modified the sequence length of the calibration dataset from 256 to 512.

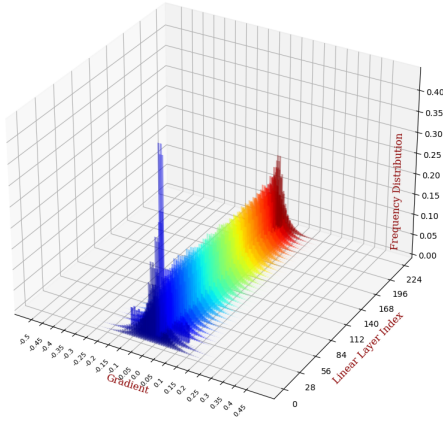
Type	Accuracy				PPL on C4			
	LLaMA		OPT		LLaMA		OPT	
Size	30b	65b	30b	66b	30b	65b	30b	66b
FP16	73.46	75.48	67.87	69.54	6.13	5.98	11.46	10.99
RTN	72.33	73.91	65.94	37.12	6.54	6.46	13.56	305.73
GPTQ	72.85	<b>74.45</b>	<b>67.55</b>	68.23	<b>6.42</b>	<b>6.23</b>	<b>11.59</b>	<b>11.24</b>
Ours	72.69	74.02	66.74	68.80	6.47	6.34	11.84	11.42
Ours-seq512	<b>72.86</b>	73.91	67.40	<b>69.22</b>	6.47	6.44	11.77	11.45

### A.4 VIEW OF V

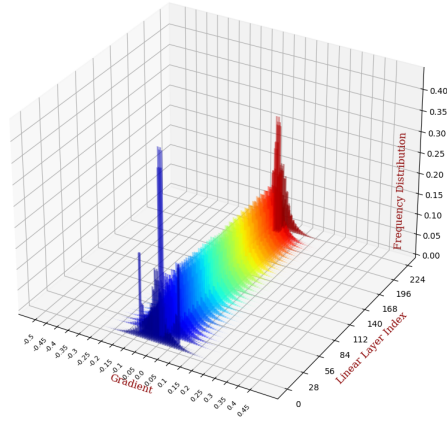
We provide an analysis of the magnitude distribution of  $V$  in Eq. 2 for approximately 7B models at W4 in Figure 4. The findings reveal that the majority of  $V$  values are concentrated within the range of  $[-0.3, 0.3]$ . Notably, the middle layers demonstrate a narrower distribution in comparison to the other layers. This observation suggests that the head or tail layers may be more susceptible to the compression.

Table 10: Wikitext ppl( $\downarrow$ ) for LLaMA & OPT with size  $\geq 30$ B. "Ours-seq512" indicates that we have modified the sequence length of the calibration dataset from 256 to 512.

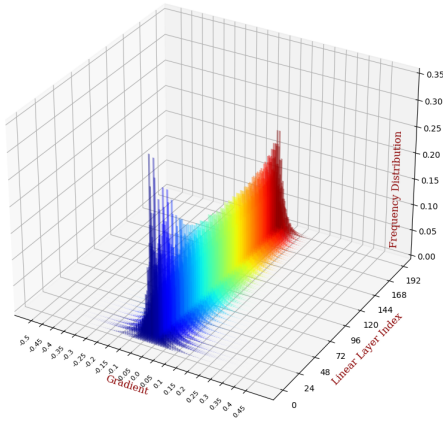
Type	W4				W3G128			
	LLaMA		OPT		LLaMA		OPT	
Size	30b	65b	30b	66b	30b	65b	30b	66b
FP16	4.10	3.56	9.56	9.34	4.10	3.56	9.56	9.34
RTN	4.54	3.99	10.98	110.43	4.87	4.44	23.05	126.92
GPTQ	<b>4.45</b>	4.16	<b>9.66</b>	9.66	4.84	4.17	<b>9.75</b>	<b>10.58</b>
Ours	4.51	3.91	9.88	<b>9.56</b>	4.85	<b>4.15</b>	11.07	11.87
Ours-seq512	4.52	<b>3.90</b>	9.88	9.70	<b>4.81</b>	4.17	10.54	10.84



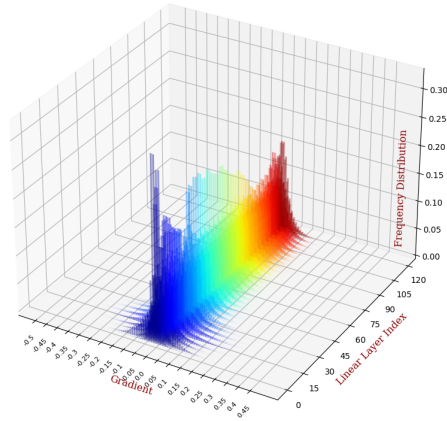
LLaMA-7B



LLaMA-7B-V2



Opt-6.7B



BLOOM-7B1

Figure 4: The distribution of the magnitude of  $V$  in Eq. 2 for different models, namely LLaMA-7B, LLaMA-7B-V2, OPT-6.7B, and BLOOM-7B1 at W4. Each color in the distribution represents a specific layer index in the models, with blue indicating shallow layers closer to the data layer, and red representing deeper layers.